Energy & Environmental Science

PAPER

View Article Online
View Journal | View Issue

Cite this: *Energy Environ. Sci.*, 2015, **8**, 617

Adipic acid production from lignin†

Derek R. Vardon,‡[ab] Mary Ann Franden,‡[a] Christopher W. Johnson,‡[a] Eric M. Karp,‡[a] Michael T. Guarnieri,[a] Jeffrey G. Linger,[a] Michael J. Salm,[a] Timothy J. Strathmann[b] and Gregg T. Beckham*[a]

Received 13th October 2014
Accepted 11th December 2014

DOI: 10.1039/c4ee03230f

www.rsc.org/ees

Lignin is an alkyl-aromatic polymer present in plant cell walls for defense, structure, and water transport. Despite exhibiting a high-energy content, lignin is typically slated for combustion in modern biorefineries due to its inherent heterogeneity and recalcitrance, whereas cellulose and hemicellulose are converted to renewable fuels and chemicals. However, it is critical for the viability of third-generation biorefineries to valorize lignin alongside polysaccharides. To that end, we employ metabolic engineering, separations, and catalysis to convert lignin-derived species into *cis*,*cis*-muconic acid, for subsequent hydrogenation to adipic acid, the latter being the most widely produced dicarboxylic acid. First, *Pseudomonas putida* KT2440 was metabolically engineered to funnel lignin-derived aromatics to *cis*,*cis*-muconate, which is an atom-efficient biochemical transformation. This engineered strain was employed in fed-batch biological cultivation to demonstrate a *cis*,*cis*-muconate titer of 13.5 g L^{-1} in 78.5 h from a model lignin-derived compound. *cis*,*cis*-Muconic acid was recovered in high purity (>97%) and yield (74%) by activated carbon treatment and crystallization (5 °C, pH 2). Pd/C was identified as a highly active catalyst for *cis*,*cis*-muconic acid hydrogenation to adipic acid with high conversion (>97%) and selectivity (>97%). Under surface reaction controlling conditions (24 °C, 24 bar, ethanol solvent), purified *cis*,*cis*-muconic acid exhibits a turnover frequency of 23–30 s^{-1} over Pd/C, with an apparent activation energy of 70 kJ mol^{-1}. Lastly, *cis*,*cis*-muconate was produced with engineered *P. putida* grown on a biomass-derived, lignin-enriched stream, demonstrating an integrated strategy towards lignin valorization to an important commodity chemical.

Broader context

Lignin is an underutilized resource in fuel and chemical production from lignocellulosic biomass due to its heterogeneous nature, but its valorization is essential to the development and success of the biofuels industry. Here we demonstrate the biochemical conversion of lignin-derived monomers to *cis*,*cis*-muconate, which can then be separated from the culture media and catalytically converted into adipic acid, the most prevalent dicarboxylic acid produced from petroleum today. Integrated process demonstrations of this nature will be necessary for the continued drive towards lignin upgrading strategies, and to expand the slate of molecules that can be produced from lignin in modern lignocellulosic biorefineries.

Introduction

Lignocellulosic biomass offers a vast, renewable resource for the sustainable production of fuels, chemicals, and materials. To date, polysaccharides have been the primary biomass fraction of interest in selective conversion processes, leaving significant opportunities for valorizing underutilized components such as lignin.[1–3] Lignin, a heterogeneous aromatic polymer, is the second most abundant biopolymer after cellulose, representing 15 to 40% dry weight of plants; despite its abundance, the inherent heterogeneity and recalcitrance of lignin typically limits its use to heat and power in biochemical conversion processes.[2,4] However, as next generation biorefineries come online to produce carbohydrate-derived fuels at commodity scale, large quantities of lignin will be generated, with recent analysis indicating that lignin valorization can play a key role for their economic viability and environmental sustainability.[1,3,5]

In nature, lignin depolymerization is accomplished primarily by powerful oxidative enzymes secreted by rot fungi and some bacteria.[6] This process releases aromatic monomers during plant cell wall deconstruction, and multiple strategies have evolved for metabolism of these aromatic species. The most studied aromatic catabolic approach employs upper pathways to channel aromatic molecules into the β-ketoadipate

[a]*National Bioenergy Center, National Renewable Energy Laboratory, Golden, CO 80401, USA. E-mail: gregg.beckham@nrel.gov*

[b]*Department of Civil and Environmental Engineering, University of Illinois at Urbana-Champaign, Urbana, IL 61801, USA*

† Electronic supplementary information (ESI) available. See DOI: 10.1039/c4ee03230f

‡ Authors contributed equally to this work.

pathway *via* central intermediates, such as catechol and protocatechuate.[7,8] This strategy offers a direct means to upgrade a heterogeneous slate of lignin-derived aromatic species *via* a "biological funneling" approach.[9]

Catechol is a primary central intermediate from the upper pathways into the β-ketoadipate pathway. Many aromatic-catabolizing organisms employ a catechol-1,2-dioxygenase enzyme to ring open catechol to *cis*,*cis*-muconate (hereafter referred to as muconic acid or muconate), which is a promising intermediate for commodity chemicals. Muconate is situated well before aromatic-derived species enter central carbon metabolism (*i.e.*, the tricarboxylic acid (TCA) cycle), allowing for much greater atom efficiencies compared to products derived from acetyl-CoA (*e.g.*, lipids, polyhydroxyalkanoates), the latter which require additional metabolic steps that divert carbon to microbial biomass production and CO_2. Previous demonstrations for biological production of muconate *via* catechol ring-opening have focused on food-grade or single feedstocks, such as glucose,[10,11] benzoate,[12] catechol,[13] and styrene.[14]

Muconic acid can be converted into myriad downstream products, including adipic acid, which is the most commercially important dicarboxylic acid.[15] Adipic acid has a market volume of 2.6 million tons per year with an annual demand growth forecast of 3–3.5% globally.[16] It has uses as a polymer precursor for nylon, plasticizers, lubricants, and polyester polyols.[15,17] Conventional adipic acid production involving nitric acid oxidation of benzene is highly damaging to the environment.[15] However, a recent analysis of biorefinery lignin utilization for adipic acid production points to major economic and greenhouse gas offsets using an integrated biological and chemical catalysis approach.[5]

To effectively convert lignin to adipic acid, the development of integrated downstream separations and catalysis, alongside metabolic engineering, will be critical for commercially viable technologies, as illustrated in Fig. 1. Separation processes alone have been estimated to account for up to 60% of the final product cost for sugar-derived fermentation acids, such as lactic acid and succinic acid, a scenario likely to be encountered with muconic acid as well.[18] Likewise, the impact of trace fermentation impurities unique to lignin in downstream separations and catalysis has yet to be explored. To date, only demonstration reactions have been performed for the catalytic reduction of glucose-derived muconic acid to adipic acid,[10,11] and questions remain regarding catalyst activity screening, the impact of upstream separations, and the intrinsic activity parameters under surface reaction controlling conditions.

Here, we demonstrate an integrated scheme for the conversion of lignin to adipic acid *via* biologically derived muconic acid. Specifically, we engineered *P. putida* KT2440 to funnel lignin-derived aromatics to muconate as the organism is amenable to genetic manipulation, tolerant to a wide variety of physical and chemical stresses, and capable of utilizing numerous lignin-derived aromatic molecules.[19] To purify muconic acid from culture media, we leveraged the ring-opened aliphatic structure of muconic acid relative to aromatic feedstocks and metabolic intermediates *via* preferential adsorption of the latter, followed by low temperature and pH crystallization.[20] Noble metal catalysts were screened for muconic acid hydrogenation, and the most active formulation was evaluated under surface reaction controlling conditions to estimate the turnover frequency and apparent activation energy. Lastly, muconate was produced biologically from a corn-stover derived, lignin-enriched stream, serving as proof-of-concept for an integrated biological and chemical lignin valorization process.

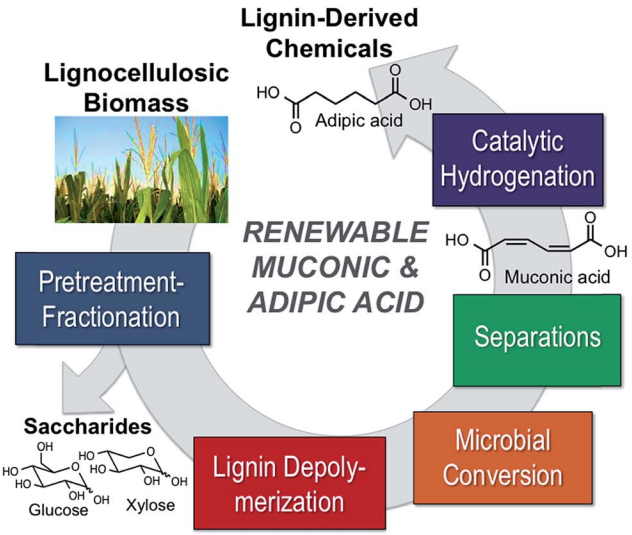

Fig. 1 Integrated biorefinery process scheme to produce muconic acid and adipic acid from lignin. Alkaline pretreatment fractionates biomass and depolymerizes lignin to produce an aromatic-rich aqueous stream. Engineered *P. putida* then biologically funnels lignin-derived aromatics to muconate, which is purified and separated. Lastly, catalytic hydrogenation converts muconic acid to adipic acid, demonstrating a new class of lignin-derived commodity chemicals.

Results

Metabolic engineering for muconate production

Muconate is produced natively in *P. putida* by the action of a catechol-1,2-dioxygenase enzyme as an intermediate in the catechol branch of the β-ketoadipate pathway.[19] Protocatechuate is metabolized *via* another branch of the β-ketoadipate pathway that does not include muconate as an intermediate. Given that many lignin-derived species will be funneled through one of these two central aromatic intermediates, our metabolic engineering strategy aimed to convert aromatics from both the catechol and protocatechuate branches of the β-ketoadipate pathway to muconate, as shown in Fig. 2. To capture aromatic species that are metabolized through protocatechuate, *pcaHG*, which encodes a protocatechuate 3,4 dioxygenase, was replaced with *aroY*, encoding a protocatechuate decarboxylase from *Enterobacter cloacae*[21] (ESI Fig. S1A†) using a marker-free homologous recombination system.[22,23] This enabled the conversion of protocatechuate and upstream metabolites to catechol, while simultaneously eliminating further catabolism of protocatechuate to β-ketoadipate.

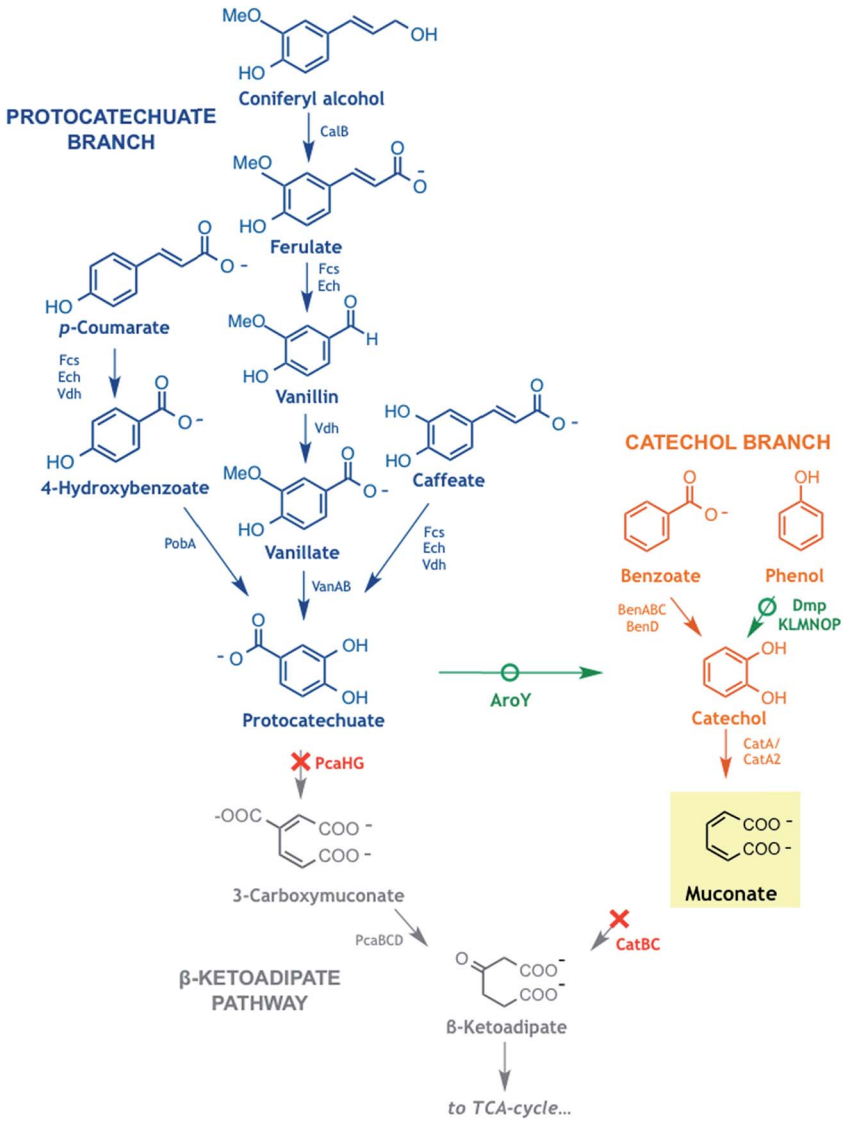

Fig. 2 Biological funneling of lignin aromatics to muconate. *P. putida* KT2440 was engineered to delete genes encoding PcaHG and CatBC (red crossed arrow) and insert genes encoding AroY and DmpKLMNOP (green circled arrow), enabling biological funneling of diverse lignin-derived monomers to muconate.

P. putida was then engineered to expand substrate utilization and to eliminate further metabolism of muconate. Intradiol ring opening of catechol to muconate is accomplished by two redundant dioxygenases, CatA and CatA2. CatA is encoded along with CatB and CatC, the next two enzymes in the catechol branch of β-ketoadipate pathway, in an operon regulated by CatR, a LysR family transcriptional regulator.[24] In order to eliminate further metabolism of muconate and enable strong, constitutive expression of CatA, a genomic section containing *catR*, *catBC*, and the promoter for *catBCA* was replaced with the tac promoter.[25] Lastly, as phenol is a commonly-derived lignin intermediate, we integrated the genes encoding the phenol monooxygenase from *Pseudomonas sp.* CF600,[26] *dmpKLMNOP*, downstream of *catA* to form an operon driven by the tac promoter (ESI Fig. S1B†).

The metabolic performance of the engineered *P. putida* strain, KT2440-CJ103, was evaluated in shake-flask experiments to demonstrate substrate utilization and production of muconate from model lignin-derived monomers, using acetate as a carbon and energy source (Fig. 3A, further details provided in ESI Fig. S2†). KT2440-CJ103 successfully produces muconate from catechol, phenol, and benzoate *via* the catechol branch, as well as from protocatechuate, coniferyl alcohol, ferulate, vanillin, caffeate, *p*-coumarate, and 4-hydroxybenzoate *via* the protocatechuate branch. We observed muconate yields ranging from 14% with coniferyl alcohol to 93% with benzoate. For compounds metabolized through vanillate (coniferyl alcohol, ferulate, and vanillin), yields were quite low with substantial accumulation of the intermediate vanillate, likely due to regulation as discussed below. In contrast, for compounds metabolized through the catechol branch (phenol, catechol,

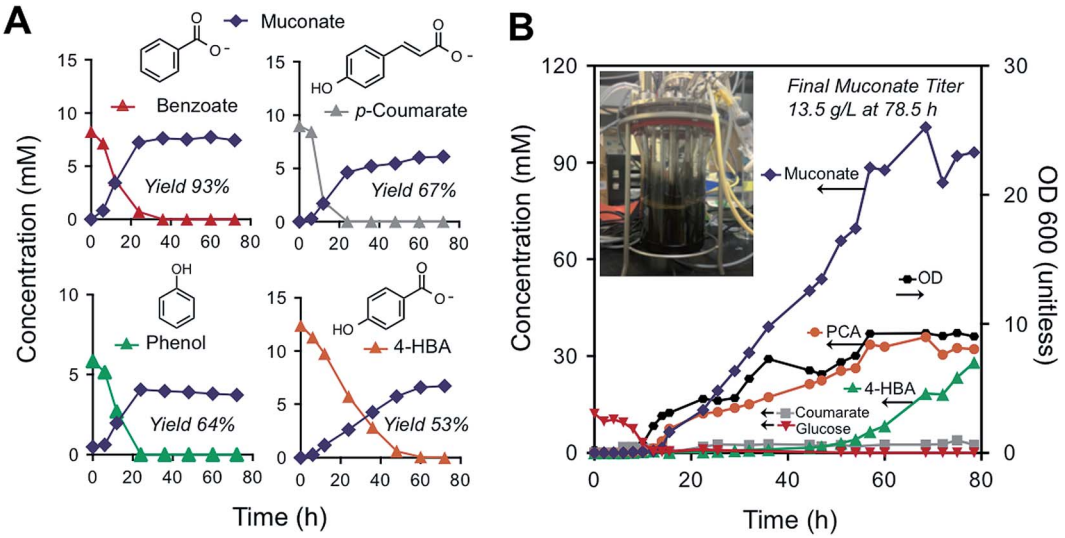

Fig. 3 Biological conversion of lignin-derived aromatics to muconate. (A) Shake flask experiments using *P. putida* KT2440-CJ103 to convert benzoate, *p*-coumarate, phenol, and 4-hydroxybenzoate (4-HBA) to muconate. (B) DO-stat fed-batch cultivation of *P. putida* KT2440-CJ103 using glucose as a carbon source to convert *p*-coumarate to muconate. Horizontal arrows indicate corresponding axis for tracked compounds and optical density at 600 nm (OD 600).

benzoate), as well as *p*-coumarate and 4-hydroxybenzoate, yields were significantly higher. Lastly, substrate loss from abiotic oxidation (data not shown) contributed to reduced yields from caffeate, and to a lesser extent, catechol. Additional experiments to test the influence of glucose or acetate as a co-fed carbon source for energy and cell growth showed higher muconate yields from cultures grown on glucose, likely due to the additional reducing equivalents and ATP generated by glucose metabolism (ESI Table S3†).

Fed-batch biological conversion with *p*-coumarate

We next sought to demonstrate the performance of the engineered strain in a fed-batch bioreactor experiment, expecting that greater production of muconate could be achieved with increased aeration, pH control, and a metered dosing of substrates for growth and conversion. Dissolved oxygen static (DO-stat) fed-batch biological conversion by KT2440-CJ103 yielded a muconate titer of 13.5 g L^{-1} after 78.5 h using *p*-coumarate as a model lignin monomer substrate, over 15 times greater than shake flask results (Fig. 3B). Preliminary experiments indicated that muconate production from *p*-coumarate was significantly inhibited in the presence of excess glucose or acetate, potentially due to catabolite repression control or other regulatory inhibition.[27–29] Therefore, DO-stat was used to maintain glucose levels below 1 mM (ref. 30) and co-feed *p*-coumarate and ammonium sulfate (ESI Fig. S3†). During the course of cultivation, protocatechuate buildup occurred. Moreover, as the cultivation progressed past 60 h, muconate levels plateaued and 4-hydroxybenzoate, a metabolite upstream of protocatechuate, accumulated. The color of the culture medium darkened over time, as shown in Fig. 3B, first panel. It may be possible to achieve higher yields with less by-product formation *via* strain development and process optimization, as discussed below.

Separation and recovery of muconic acid

To ultimately produce high-purity adipic acid as a final product from lignin, our next goal was to recover muconate selectively from cell-free culture media as impurities resulting from biological conversion media and aromatic intermediates will undoubtedly affect the quality and performance of adipic acid during polymerization or subsequent chemical transformations. The biological ring opening of muconate allowed for facile purification from culture media containing non-target aromatic metabolites (*e.g.*, protocatechuate and 4-hydroxybenzoate) using activated carbon due to the high adsorption affinity of oxygenated aromatics in comparison to aliphatic acids.[31,32] After adding activated carbon to the culture media at 12.5% (wt/vol) with stirring for 1 h,[33] nearly complete removal (below detectable limit by HPLC) of protocatechuate and 4-hydroxybenzoate was achieved, while the majority of muconate (89% of initial culture media concentration, mass/vol) remained in solution (Fig. 4). Muconic acid was then crystallized by reducing the pH and temperature, following from the strong pH and temperature dependence of dicarboxylic acids.[33,34] At pH 2 and 5 °C, muconic acid readily precipitated from solution and crystals were recovered by vacuum filtration. This method recovered 74% of the muconic acid in the purified broth with a high degree of purity (>97%), as shown in Fig. 3.

Catalytic hydrogenation of muconic acid to adipic acid

Catalyst screening experiments were then conducted to identify highly active materials for muconic acid hydrogenation at low temperature and pressure. Commercial noble metal catalysts supported on carbon were initially tested at 5 wt% loading, including Pd, Pt, and Ru. Characterization of the virgin catalyst materials (Fig. 5A, ESI Table S4†) revealed the metals were dispersed as small crystallites, with comparable support surface

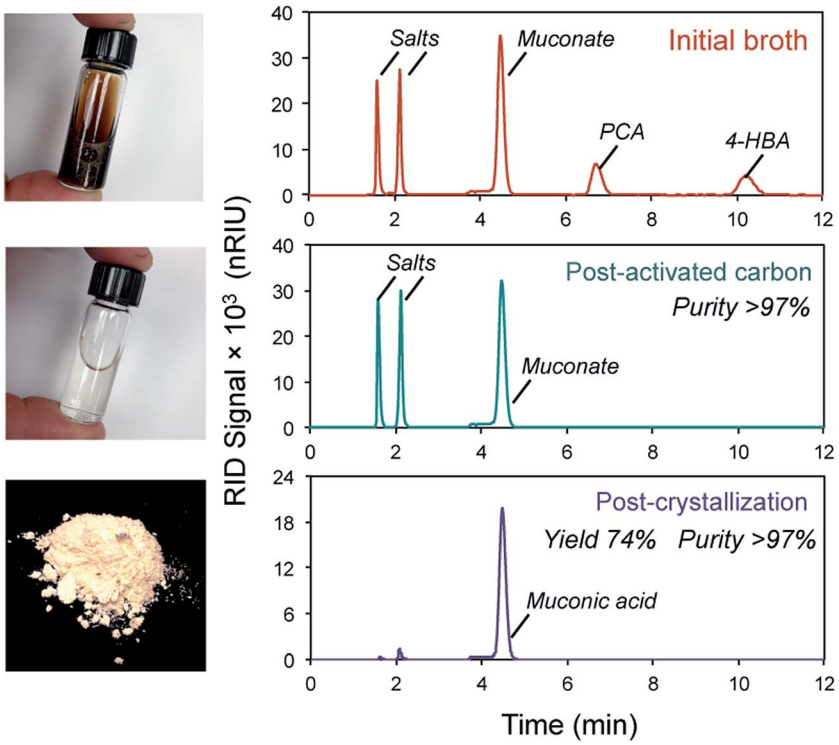

Fig. 4 Separation of muconic acid following fed-batch biological conversion of *p*-coumarate. Fed-batch culture broth containing muconate derived from *p*-coumarate was purified using activated carbon to remove aromatic metabolic intermediates, which consisted primarily of protocatechuate (PCA) and 4-hydroxybenzoate (4-HBA). Following purification, muconic acid was recovered in high yield (74%) and purity (>97%) by crystallization at reduced pH and temperature (pH 2, 5 °C).

areas (705–1075 $m^2\ g^{-1}$), pore volumes (0.51–0.71 mL g^{-1}), and a wider range of exposed active metal areas (22–51% dispersion). Screening experiments found that Pd/C was by far the most active catalyst, with consistent activity trends when using M9 culture media (aqueous solution containing salts to support biological growth) or ethanol, as a representative protic polar organic solvent (ESI Fig. S4†). During the course of the reaction, 2-hexenedioc acid was observed as the primary intermediate, likely due to the low temperature conditions that minimized competing nonselective reaction pathways (ESI Fig. S5†). For reactions that went to completion with Pd, selectivity to adipic acid was >97% (mol mol^{-1}) (Fig. 5B).

Additional hydrogenation conditions were examined with Pd/C to (i) determine its activity under surface reaction controlling conditions, (ii) evaluate the apparent activation energy for muconic acid reduction, and (iii) demonstrate its utility with muconic acid recovered from fed-batch biological conversion. Experiments conducted at two different Pd loadings (1 wt% and 2 wt% Pd/C) exhibited comparable turn over frequencies (TOF; 23 ± 6 s^{-1} and 30 ± 6 s^{-1}, respectively, at 24 bar of hydrogen and 24 °C in ethanol), supportive of surface reaction controlling conditions by the Koros–Nowak criterion (ESI Fig. S6†).[35] Experiments to measure the hydrogenation rate of muconic acid at varying temperatures estimated an apparent activation energy of ~70 kJ mol^{-1} (Fig. 5C, ESI Fig. S7†), significantly above values indicative of mass transfer limitation (<20 kJ mol^{-1}).[36] Hydrogenation with Pd/C was then demonstrated with muconic acid obtained from fed-batch biological conversion of *p*-coumarate after activated carbon purification and crystallization. Hydrogenation at room temperature progressed rapidly in a series reaction (Fig. 5D, muconic acid TOF 25 ± 3 sec^{-1}), resulting in high purity adipic acid as the final product (>97% mass/mass). Variability in sample mass closure was attributed to error introduced during sampling and filtration of reactor contents prior to analysis, as well as potential adsorption of organics to the catalyst carbon support, with individual species concentrations and molar closure provided in ESI Table S5.† After the reaction, analysis of the ethanol solvent indicated that leaching of Pd occurred to a minor extent (7 μg L^{-1}, 0.8% of the loaded metal), which can occur due to the acidic liquid phase conditions employed.[37]

Biological conversion of depolymerized lignin

Lastly, as an initial proof of concept for this process scheme, muconate was produced from biomass-derived lignin in shake flask conditions. Namely, alkaline pretreatment with NaOH and anthraquinone (AQ) was applied to corn stover at 70 mg NaOH/g dry biomass with an AQ concentration of 0.2 wt% of dry stover, in a manner similar to our previous work.[9,38] The resulting alkaline pretreated liquor (APL) stream contains a substantial amount of lignin-derived aromatics, acetate, biomass extractives, and very minor concentrations of sugars (<0.5 g L^{-1} of any monomeric sugar).[9,38] The pH of APL was reduced to 7 with the addition of H_2SO_4. The liquor was then filtered through a 0.2 μm filter for sterilization and to remove residual solids.

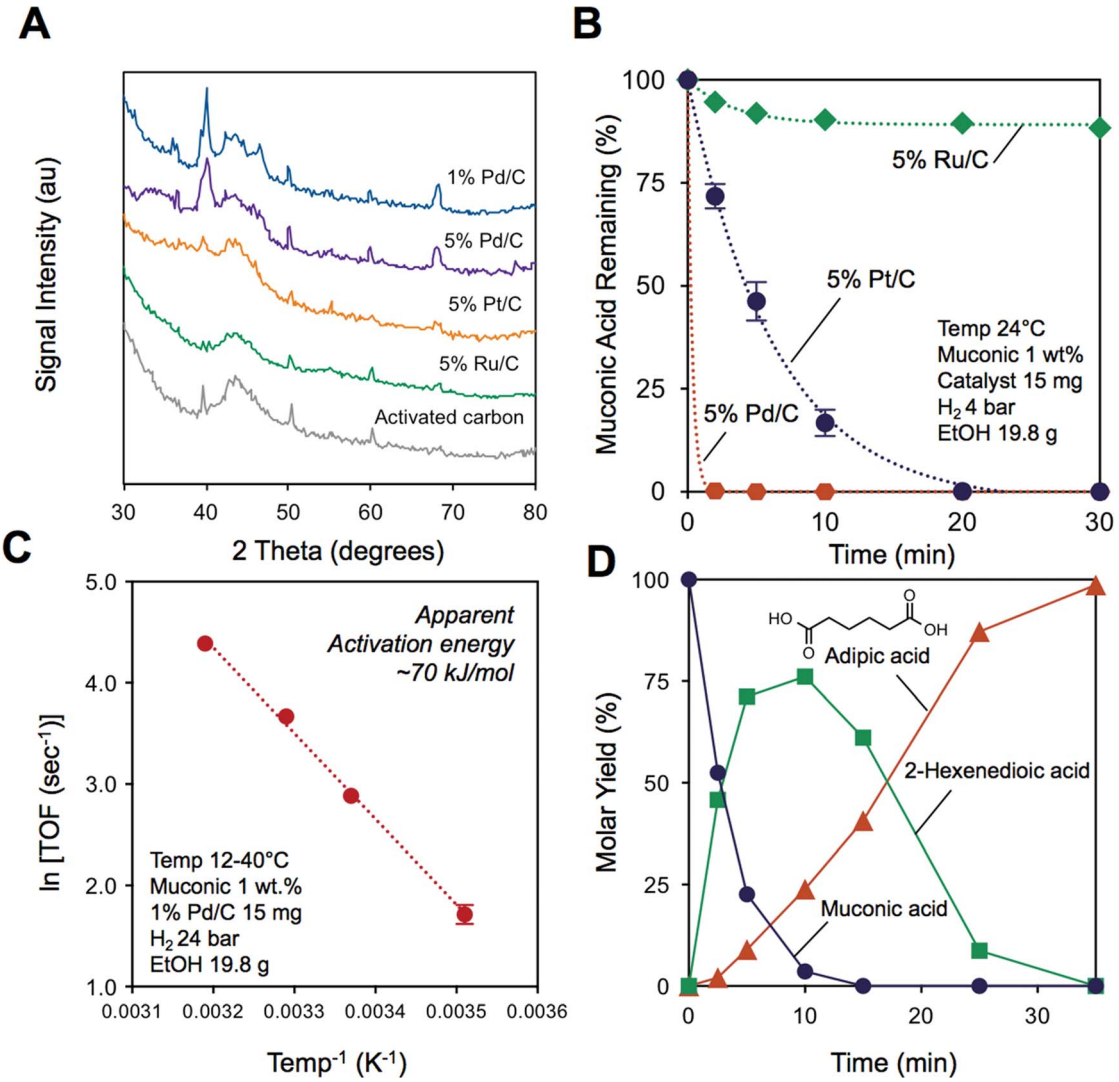

Fig. 5 Catalytic hydrogenation of muconic acid to adipic acid. (A) X-ray diffraction analysis of commercial catalysts confirmed metals were highly dispersed as small crystallites, with additional material properties described in the ESI.† Variations in XRD spectra with the carbon support were attributed to materials obtained from differing vendors. (B) Noble metal catalysts were first screened with purified muconic acid obtained commercially for hydrogenation to adipic acid under mild conditions, with pseudo-first order kinetic parameter fits indicated by dashed lines. Reactions were performed in triplicate, with error bars indicating the conversion standard deviation. (C) The activity of commercial 1% Pd/C was evaluated under surface reaction controlling conditions to estimate the apparent activation energy for muconic acid hydrogenation in ethanol (EtOH) using the Arrhenius equation. (D) Catalytic conversion of muconic acid derived from fed-batch biological conversion of *p*-coumaric acid following activated carbon purification and crystallization. Reaction conditions were as follows: temperature 24 °C, muconic acid 200 mg, commercial 1% Pd/C 15 mg, H_2 pressure 24 bar, EtOH solvent 19.8 g. Typical mass closure was >97%, with species concentrations shown in ESI Table S4.†

Flasks containing 25 mL M9 minimal medium supplemented with 0.9X APL were then inoculated with *P. putida* KT2440 or KT2440-CJ103 and cultured for three days. Following biological conversion, cells were removed by centrifugation and activated carbon (12.5 wt/vol%) was added to the remaining culture media to remove non-target aromatics and facilitate analysis by HPLC. The complexity and pH sensitivity of APL impedes direct quantitative compositional analysis by conventional methods;[39] however, analysis by HPLC detected significant levels of muconic acid in cultures grown with *P. putida* KT2440-CJ103, while no significant quantities were detected in the blank APL control sample or with the native *P. putida* KT2440 (Fig. 6A). Likewise, analysis of derivatized acids in unpurified culture samples by GC × GC-TOFMS (time-of-flight mass spectrometry) confirmed the identity of muconic acid and displayed comparable trends in concentration, as shown in of Fig. 6B.

To track the conversion of primary aromatic and nonaromatic components in APL during shake flask cultivation, GC × GC-TOFMS was also employed. Analysis of APL determined that *p*-coumarate and ferulate were initially present at significant levels (0.92 g L^{-1} and 0.34 g L^{-1}, respectively), in addition to the short chain acids glycolate and acetate (0.46 g L^{-1} and 0.10 g L^{-1}, respectively), as shown in Fig. 6C. Other aromatic acids, including benzoate, caffeate, vanillate, and 4-hydroxybenzoate, were not detected in significant levels (>0.01 g L^{-1}). During shake flask cultivations, *P. putida* KT2440-CJ103 rapidly consumed glycolate

and acetate, which can be used as sources of carbon and energy for growth. The primary aromatic components, *p*-coumarate and ferulate, were converted to 0.70 g L^{-1} of muconate after 24 h (Fig. 6C). Based on the consumption of these two major aromatic acids, the molar yield to muconate was 67% (Fig. 6).

Discussion

Techno-economic analysis has suggested that lignin valorization will become essential for the production of advanced biofuels.[5] As recently reviewed,[1] lignin valorization will be enabled by many different technological advances including genetic modifications of plants,[40–43] new biomass pretreatment and depolymerization technologies,[3,38,44–47] tailored separation processes,[48] and catalytic product-slate diversification. Leveraging these developments for lignin valorization holds potential to capitalize on the unique aromatic functionality that greatly differentiates lignin from polysaccharides. Almost invariably, lignin depolymerization strategies result in a multitude of aromatic compounds.[1,3,49] Tasking

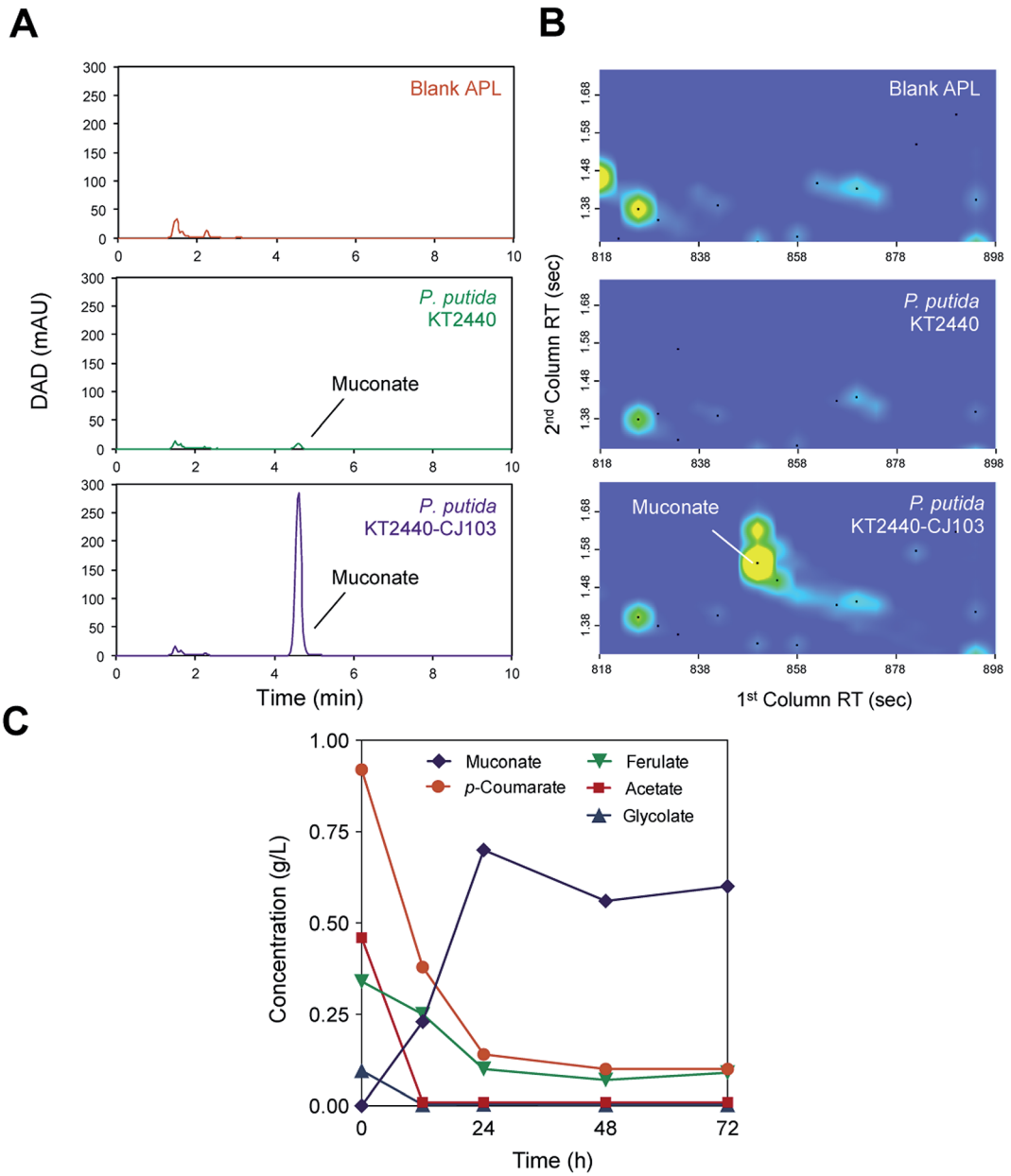

Fig. 6 Biological production of muconate from a depolymerized lignin stream. (A) HPLC analysis of culture media purified by activated carbon confirmed that alkaline pretreated liquor (APL) was converted to muconic acid after 72 h by the engineered strain *P. putida* KT2440-CJ103, while no significant quantities were detected using the native organism *P. putida* KT2440 or in blank APL. (B) GCxGC-TOF-MS analysis of derivatized acids in the unpurified culture samples confirmed the identity of muconic acid, with comparable trends in concentration. (C) Shake flask cultivation with *P. putida* KT2440-CJ103 in APL demonstrated that major aromatic acids and short chain acids were metabolized, producing a maximum muconate concentration of 0.70 g L^{-1} after 24 h.

microorganisms to funnel these heterogeneous organic molecules to simplified product streams can potentially overcome this limitation,[9] but significant considerations remain to realize this general approach.

Efficient conversion of substrate to product and high product yields are of crucial importance for economically viable biomass upgrading strategies. Unlike molecules targeted as products for biomass upgrading that are derived from pyruvate (ethanol, lactic acid), acetyl-CoA (fatty acids, wax esters, PHAs), or the TCA cycle (succinic acid), production of muconate occurs upstream of central carbon metabolism and thus is not subject to the competing interests of a growing cell that result in losses in carbon due to CO_2 and biomass production. Namely, conversion of aromatic molecules to muconate at high yields can occur concomitant with growth on non-aromatic substrates, such as acetate or glucose as demonstrated here. Indeed, yields from benzoate in our shake flask studies were 93% of the theoretical maximum.

Some other aromatic substrates, however, were not converted as efficiently, resulting in lower yields and the accumulation of intermediates such as protocatechuate, 4-hydroxybenzoate, and vanillate. It is likely that some of this accumulation is the result of transcriptional or translational regulation of enzymes in these pathways. It is well known that many of the aromatic degradation pathways involved in the production of muconate are controlled by transcriptional regulators.[8,50] While *catR* has been deleted in the production strain reported in this study, other transcriptional regulators such as BenR and VanR are likely to have contributed to accumulation of intermediates. It is also likely that transcription or translation of some of the enzymes involved are regulated, either directly or indirectly, by the Crc (catabolite repression control) protein. Crc is a global translational regulator that binds to specific RNA sequences to inhibit translation of targeted mRNAs and has been shown to regulate induction and repression of the catabolic pathways of amino acids, sugars, hydrocarbons, or aromatic compounds.[27–29] If transcriptional and/or translational regulation is a contributing factor in the accumulation of intermediates observed here, further engineering could be employed to affect expression of regulatory proteins or alter the binding targets of such proteins.

In addition to transcriptional and translational regulation, the enzymes involved could also be limited by kinetics or the thermodynamics of the reactions they catalyze. The protocatechuate decarboxylase, being an exogenous enzyme that is constitutively expressed in *P. putida* KT2440-CJ103, should not be regulated in transcription or translation. Nonetheless, an accumulation of protocatechuate was observed when producing muconate. This accumulation occurs in absence of an accumulation of the product, catechol, suggesting that equilibrium limitations are not present. Based on these observations, we hypothesize that either the specific activity of this protocatechuate decarboxylase is insufficient and/or that this enzyme is inhibited by muconic acid. Increasing the gene dosage of *aroY* or increasing the specific activity of the enzyme using protein engineering could be useful strategies for overcoming the accumulation of protocatechuate.

Finally, abiotic factors could also affect the conversion of these aromatic molecules to muconic acid. As mentioned previously, many of the cultures become darker with time. Indeed, in the absence of cells, the concentrations of some of the aromatic molecules decrease substantially in M9 minimal medium on similar time scales to the cultivation experiments and these solutions darken (data not shown). Oxidation products were not detected using the analytical methods described here, but the dark color of the spent media and the inability in some cases to account for all of the carbon metabolized by adding the muconic acid product with the intermediates accumulated suggests abiotic oxidation likely contributed to the lower yields observed in some cases. Further optimization of growth conditions might be useful in minimizing this oxidation, while increasing the activity of the individual enzymes may reduce the accumulation of intermediates that are likely to oxidize.

Regarding muconate production from biomass-derived lignin, further optimization of lignin depolymerization and bioprocess engineering, in addition to the metabolic engineering strategies discussed above, can provide a direct path forward for industrially relevant productivities and yields. In the current study, a biomass-derived, lignin-enriched substrate, APL, was used.[38] Alkaline treatment of biomass is typically used either in pulping to delignify biomass (at high severity), or as a pretreatment strategy to remove acetate and partially delignify biomass (at low severity).[38,51] However, in both cases, the resulting black liquor is not traditionally slated for subsequent upgrading. Thus, optimization of the alkaline pretreatment step has not been thoroughly conducted to our knowledge to yield a substrate with sufficiently high monomer concentrations required for industrially relevant biological conversion to muconate. With regards to bioprocess engineering, previous studies on non-lignin substrates have demonstrated that substantial process improvements can be achieved through control of substrate, growth media, and oxygen delivery.[11,30,52] As such, coupled optimization of all aspects will be required to achieve industrially relevant muconate titer, productivity, and yield from lignin-derived substrates.

In addition to improving yields during biological conversion, cost-effective separation strategies will be essential for valorizing lignin due to the necessary high carbon-to-product yield and purity requirements for renewable commodity chemicals. As noted previously, separation of biologically produced acids has been estimated to account for over 60% of production costs.[18] Selection of metabolic pathways that dramatically alter the chemical functionality of the parent lignin monomer (*e.g.*, oxidative ring-opening to dicarboxylic acids) and its physicochemical properties (*e.g.*, solubility, pK_a)[48] can greatly reduce the process intensity for separations. As demonstrated with the fed-batch conversion of *p*-coumaric acid, selective adsorption of non-target aromatic metabolites with activated carbon provides a facile mechanism for purifying muconic acid. Development of novel adsorbents that allow for non-target metabolite release and recycle can also maximize carbon utilization efficiency, similar to strategies being examined for oil spill remediation.[53] After purification, crystallization of muconic acid retains highly

soluble salts and low molecular weight acids in the aqueous phase, minimizing the impact of impurities on downstream catalysis and end product purity. Although a fraction of muconic acid remained soluble in the culture media (~3.4 g L^{-1}) at low temperature and pH, higher titers in the culture media can greatly improve the fractional recovery by crystallization, which will be pursued in future studies.

As illustrated in this work, biological funneling can greatly simplify downstream catalytic processing for valorizing lignin as it can yield single intermediates.[9] Target compounds from biological conversion can be judiciously selected to ensure catalytic pathways are atom efficient, while maintaining the high degree of chemical functionality inherent to biomass.[54] This is exemplified with muconic acid, in which the dicarboxylic functionality is retained for purposeful end-use as a polymer precursor, *in lieu* of full deoxygenation to hydrocarbon fuels. As demonstrated in this and previous efforts,[10,11] hydrogenation of muconic acid to adipic acid is nearly quantitative at mild temperatures, greatly reducing catalytic process intensity.

Within the framework of integrated bio-catalytic processing, advancements in catalyst design and engineering can also accelerate the use of lignin as feedstock for renewable chemical production. Knowledge regarding the activity and stability of conventional noble metals for muconic acid hydrogenation can provide a baseline for improved catalyst design. In worldwide catalysis efforts, material substitutes are currently being developed for platinum group metals to achieve comparable activity for chemistries critical to biomass valorization. Strategies include alloying primary metals with low-cost secondary metals,[55,56] utilizing earth abundant metal oxides and carbides,[57,58] and enhancing activity and selectivity through tailored synthesis of metal crystallite size, shape, and facets.[59,60] In addition to material design, knowledge regarding the activity of these catalysts in solvent systems compatible with separation processes and their sustained performance in the presence of residual impurities from biological conversion will be key to their development and implementation at scale.

Conclusion

Lignin has typically been viewed as a small volume or niche feedstock, such as for the production of vanillin or lignosulfonates, given its intrinsic heterogeneity and recalcitrance. In the context of biofuels production, lignin is currently seen through a similar lens, with initial biorefinery designs slating lignin for heat and power despite having a higher energy density and C : O ratio than polysaccharides. However, recent economic and environmental analysis has shown that lignin valorization will be an essential component of next generation lignocellulosic biorefining.[5] To that end, here we have demonstrated an integrated strategy to combine biological funneling, separations, and chemical catalysis to produce adipic acid from lignin-derived aromatic molecules. More broadly, the ability to funnel a heterogeneous mixture of lignin-derived species coupled to the use of a tunable biocatalyst, tailored separations, and catalytic upgrading will enable the production of targeted, single intermediates with high atom efficiency, thus overcoming the intrinsic heterogeneity of lignin – the primary technical hurdle in lignin valorization. This overall co-design concept for lignin valorization offers a versatile path forward for the production of fuels, chemicals, and materials from lignin.

Materials and methods

Strains, media, and growth conditions

Cells and media used for plasmid construction and gene replacements are described in ESI Methods, Fig. S1, Table S1 and S2.†

P. putida KT2440 (ATCC 47054) and its derivatives were grown shaking at 225 rpm, 30 °C, in LB Broth or LB plates. During gene replacement, sucrose selection was performed on YT+25% sucrose plates (10 g L^{-1} yeast extract, 20 g L^{-1} tryptone, 250 g L^{-1} sucrose, 18 g L^{-1} agar). Shake flask and bioreactor experiments were performed using modified M9 minimal media containing 13.56 g L^{-1} disodium phosphate, 6 g L^{-1} monopotassium phosphate, 1 g L^{-1} NaCl, 2 g L^{-1} NH_4Cl, 2 mM $MgSO_4$, 100 μM $CaCl_2$, and 18 μM $FeSO_4$. Details regarding plasmid construction and gene replacement are described in ESI Methods.†

Shake flask experiments with model monomers and APL

Fed batch and shake flask experiments were performed using 125 mL baffled flasks containing 25 mL modified M9 media supplemented with 10 mM sodium benzoate, coniferyl alcohol, ferulate, vanillin, caffeate, *p*-coumarate, 4-hydroxybenzoate or 5 mM phenol and 20 mM sodium acetate or 10 mM glucose. For shake flask experiments in which cells were grown on alkaline pretreated liquor (APL), modified M9 medium was supplemented with APL at a concentration of 0.9X.[9] Cultures were inoculated with cells washed in modified M9 medium to OD_{600} 0.05, then incubated shaking at 30 °C, 225 rpm. Every 12 hours, cultures were sampled for HPLC, OD_{600}, and pH measurement. For cultures at pH > 7.4 or < 6.6, the pH was adjusted to 7.0 by adding 1 N HCl or 1 N NaOH. 20 mM sodium acetate or 10 mM glucose was added before returning the cultures to the incubator. Substrates and products were analyzed as described in ESI Methods.†

Fed-batch fermentation

A seed batch culture of *P. putida* KT2440-CJ103 was started in a shake flask and grown overnight in LB, 30 °C, 225 rpm. The next morning, cells were centrifuged 3800 × *g*, 10′ and washed once with modified M9 medium containing 10 mM glucose. Cultures were transferred to 700 mLs of the same medium in a 2L Applikon (Applikon Biotechnology, Inc.) EZ Control 2L bioreactor, starting at an initial OD_{600} of 0.2. Base pH was controlled by 2 N NaOH to pH 7. The temperature was maintained at 30 °C. Mixed air was used to deliver oxygen at a flow rate of 2 L min^{-1}. DO saturation was manually adjusted to ~50% by varying stirrer speed, from 250 to 650 rpm, and then maintained at 650 rpm for the duration of the experiment. At 5 h, 2 mM *p*-coumarate was added. When glucose was consumed at ~11.5 h, a large spike in DO was observed, indicating that glucose was depleted

and confirmed by YSI analysis. A separate pump was computer programmed to deliver for 30 seconds (~2.4 mL) a glucose : *p*-coumarate : ammonium sulfate (68.4 : 36.5 : 9 g L^{-1}) feed when DOT (dissolved oxygen tension) levels reached ≥75%. The feed caused a temporary drop in DOT to ~50%, until glucose concentrations fell again. As expected, DOT oscillations proceeded at similar frequencies (Fig. S3†), until the glucose:*p*-coumarate:ammonium sulfate feed was terminated at 75.5 h and the bioreactor was shut down at 78.5 h.

Purification and crystallization

Fed-batch fermentation broth was initially purified to remove non-target aromatic metabolites. The broth was purified by the addition of 12.5 w/v% activated carbon (Sigma Aldrich, Darco 100 mesh) with stirring at 350 rpm for 1 h.[33] Activated carbon was removed *via* vacuum filtration (0.2 μm-PES filter assembly, Nalgene).

Muconic acid crystallization was initiated by adjusting the filtrate pH to 2 by HCl addition. The broth was chilled to 5 °C and precipitated crystals were recovered by vacuum filtration (Nalgene). Crystals were dried for 24 h in a vacuum oven and weighed, prior to analysis by HPLC. Muconic acid purity post activated carbon, recovery following crystallization, and crystal purity were calculated based on eqn (1)–(3), respectively.

$$\text{Post activated carbon purity (\%)} = \frac{\text{Muconic acid (g L}^{-1})}{\text{Total organic acids (g L}^{-1})} \times 100\% \quad (1)$$

$$\text{Crystallization recovery (\%)} = \frac{\text{Crystallized muconic acid (g)}}{\text{Muconic acid purified broth (g L}^{-1}) \times \text{Volume (L)}} \times 100\% \quad (2)$$

$$\text{Crystallization purity (\%)} = \frac{\text{Crystallized muconic acid (g)}}{\text{Crystallized solids (g)}} \times 100\% \quad (3)$$

Catalysis

Commercial monometallic noble metal catalysts were screened for their hydrogenation activity with muconic acid. Catalysts at 5 wt% loading on activated carbon were obtained from Sigma Aldrich (Pt, Pd, and Ru) and 1 wt% Pd/C was obtained from Alfa Aesar. Virgin catalyst materials were initially characterized to determine their average crystallite size and long-range order by X-ray diffraction, support surface area and pore volume by nitrogen physisorption, and active metal surface area by hydrogen chemisorption, with details described elsewhere.[61] Due to the high sensitivity of Pd dispersion with temperature,[62] Pd samples were reduced under flowing hydrogen (50 mL min^{-1}, 10% H_2 in Ar) at moderate temperature (125 °C, 3 °C min^{-1}) and held for 1 h. Following reduction, Pd samples were purged for 1 h under Ar and cooled to 45 °C prior to H_2/O_2 titration. For calculations of Pd dispersion, the amount of hydrogen uptake that followed the second oxygen titration was used. A stoichiometry of 0.667 Pd sites per H_2 molecule was assumed to remove oxidized Pd–O species in the form of water and form the reduced Pd–H species.

Hydrogenation screening experiments with 5 wt% catalysts were performed in 200 proof ethanol using a Parr 5000 Multireactor system (Parr Instruments). For model compound studies, commercial *cis*,*cis*-muconic acid (Sigma Aldrich) was initially purified using activated carbon and crystallized at low pH and temperature, as described above. Screening solvents included ethanol, as well as simulated culture media prepared with mock M9 culture media (Sigma Aldrich) adjusted to pH 7 with NaOH. Reactions were performed in triplicate using 75 mL vessels operating at 1600 rpm stirring, with hydrogen supplied at constant pressure by a distributed gas manifold operating in dead end mode. Samples were collected with an *in situ* sampling valve and syringe filtered (0.2 μm Nylon, VWR) prior to analysis by HPLC. After the reaction, leaching of Pd/C was determined by ICP-OES. The ethanol solution was vacuum filtered (0.2 μm-PES filter assembly, Nalgene) and dried under nitrogen to remove solvent prior to analysis.

Conversion of muconic acid was calculated by dividing the moles of muconic acid measured in each sample by the moles of muconic acid at time zero. Selectivity to adipic acid was calculated by dividing the moles of adipic acid measured by the moles of muconic acid converted in each sample. The reduction of muconic acid was modeled as pseudo-first order to estimate the rate constant using non-linear regression with GraphPad Prism version 6.00 (Graphpad Software). Catalyst TOF was calculated by dividing the rate of muconic acid conversion (moles of muconic acid per second, estimated using the modeled pseudo-first order rate constant at 10% muconic acid conversion) by the moles of surface exposed active metal determined by chemisorption.

To evaluate the influence of mass transfer on the observed rate of muconic acid hydrogenation, the TOF of Pd was compared at two different catalyst metal contents and at varying temperature. Pd/C catalysts were prepared in house at 1 wt% and 2 wt% metal loading by incipient wetness to evaluate their TOF by the Koros–Nowak criterion.[35] Pd-acetate (Sigma Aldrich) was dissolved in acetone and loaded onto sieved activated carbon (<270 mesh). Catalysts were dried overnight and reduced in flowing hydrogen at 125 °C for 2 h. Experiments were performed in triplicate at elevated pressure (24 bar) to facilitate hydrogen mass transfer. The activation energy for muconic acid hydrogenation was then estimated with the Arrhenius equation by varying the temperature from 12–40 °C and measuring the influence on the observed TOF with commercial 1% Pd/C obtained from Alfa Aesar. The 95% confidence intervals for the observed TOF were calculated using non-linear regression with GraphPad Prism version 6.00 (Graphpad Software).

Analysis of APL-derived muconate

Activated carbon (12.5% w/v) was added to the samples taken from shake flasks with stirring for 1 h, prior to vacuum filtration (2 μm) and analysis by HPLC. To confirm the identity of muconic acid in APL, GCxGC-TOFMS analysis was performed. Acids present in the APL culture broth were converted to their

ammonium salt form, reconstituted in pyridine and derivatized with the addition of N,O-bis(trimethylsilyl)trifluoroacetamide (BSTFA), following a method similar to the one described by Alén *et al.*[63] The derivatized acids were analyzed on a LECO Pegasus GCxGC-TOFMS system with a Gerstel autosampler. Samples were run at a 30 : 1 split ratio using helium as a carrier gas and an injection volume of 1 μL. The first dimension utilized a 10 m Restek RTX-5 column and the second column dimension utilized a 0.75 m Agilent DB-1701 column. The mass spectrum and retention time of derivatized *cis*,*cis*-muconic acid was identified using a reference standard of *cis*,*cis*-muconic acid purchased from Sigma Aldrich that was converted to its ammonium salt form, dissolved in pyridine containing an internal standard of ammonium cylcohexane carboxylate and derivatized with BSTFA. For quantification purposes, *p*-coumaric acid, ferulic acid, acetic acid and glycolic acid were also converted to their ammonium salts, reconstituted in pyridine, and derivatized with BSTFA.

Acknowledgements

We thank the US Department of Energy BioEnergy Technologies Office for funding this work. Support for DRV and TJS is also provided by the National Science Foundation (NSF-CBET-1438218 and an NSF Graduate Research Fellowship to DRV). We thank Victoria Shingler from the Department of Molecular Biology at Umeå University for providing templates for plasmid assembly, Martin Menart at the Colorado School of Mines for assistance with catalyst chemisorption measurements, Dan Ruddy at NREL for physisorption measurements, and Steve Deutch at NREL for GC × GC-TOFMS analysis. We also thank Mary Biddy and Philip Pienkos at NREL for helpful discussions.

References

1 A. J. Ragauskas, G. T. Beckham, M. J. Biddy, R. Chandra, F. Chen, M. F. Davis, B. H. Davison, R. A. Dixon, P. Gilna, M. Keller, P. Langan, A. K. Naskar, J. N. Saddler, T. J. Tschaplinski, G. A. Tuskan and C. E. Wyman, *Science*, 2014, **344**, 1246843.
2 S. P. S. Chundawat, G. T. Beckham, M. E. Himmel and B. E. Dale, *Annu. Rev. Chem. Biomol. Eng.*, 2011, **2**, 121–145.
3 J. Zakzeski, P. C. Bruijnincx, A. L. Jongerius and B. M. Weckhuysen, *Chem. Rev.*, 2010, **110**, 3552–3599.
4 M. E. Himmel, S.-Y. Ding, D. K. Johnson, W. S. Adney, M. R. Nimlos, J. W. Brady and T. D. Foust, *Science*, 2007, **315**, 804–807.
5 R. Davis, L. Tao, E. C. D. Tan, M. J. Biddy, G. T. Beckham, C. Scarlata, J. Jacobson, K. Cafferty, J. Ross, J. Lukas, D. Knorr and P. Schoen, *NREL Tech. Rep.*, 2013, 88–101.
6 Á. T. Martínez, M. Speranza, F. J. Ruiz-Dueñas, P. Ferreira, S. Camarero, F. Guillén, M. J. Martínez, A. Gutiérrez and J. C. del Río, *Int. Microbiol.*, 2010, **8**, 195–204.
7 G. Fuchs, M. Boll and J. Heider, *Nat. Rev. Microbiol.*, 2011, **9**, 803–816.
8 C. S. Harwood and R. E. Parales, *Annu. Rev. Microbiol.*, 1996, **50**, 553–590.
9 J. G. Linger, D. R. Vardon, M. T. Guarnieri, E. M. Karp, G. B. Hunsinger, M. A. Franden, C. W. Johnson, G. Chupka, T. J. Strathmann, P. T. Pienkos and G. T. Beckham, *Proc. Natl. Acad. Sci. U. S. A.*, 2014, **111**, 12013–12018.
10 K. M. Draths and J. W. Frost, *J. Am. Chem. Soc.*, 1994, **116**, 399–400.
11 W. Niu, K. M. Draths and J. W. Frost, *Biotechnol. Prog.*, 2002, **18**, 201–211.
12 C.-M. Wu, C.-C. Wu, C.-C. Su, S.-N. Lee, Y.-A. Lee and J.-Y. Wu, *Biochem. Eng. J.*, 2006, **29**, 35–40.
13 K. Gomi and S. Horiguchi, *Agric. Biol. Chem.*, 1988, **52**, 585–587.
14 C.-M. Wu, T.-H. Lee, S.-N. Lee, Y.-A. Lee and J.-Y. Wu, *Enzyme Microb. Technol.*, 2004, **35**, 598–604.
15 S. V. de Vyver and Y. Román-Leshkov, *Catal. Sci. Technol.*, 2013, **3**, 1465–1479.
16 T. Polen, M. Spelberg and M. Bott, *J. Biotechnol.*, 2012, (2), 75–84.
17 M. T. Musser, in *Ullmann's Encyclopedia of Industrial Chemistry*, Wiley-VCH Verlag GmbH & Co. KGaA, 2000.
18 I. Bechthold, K. Bretz, S. Kabasci, R. Kopitzky and A. Springer, *Chem. Eng. Technol.*, 2008, **31**, 647–654.
19 J. I. Jiménez, B. Miñambres, J. L. García and E. Díaz, *Environ. Microbiol.*, 2002, **4**, 824–841.
20 Q. Li, D. Wang, Y. Wu, W. Li, Y. Zhang, J. Xing and Z. Su, *Sep. Purif. Technol.*, 2010, **72**, 294–300.
21 T. Yoshida, Y. Inami, T. Matsui and T. Nagasawa, *Biotechnol. Lett.*, 2010, **32**, 701–705.
22 C. J. Marx, *BMC Res. Notes*, 2008, **1**, 1.
23 A. Schäfer, A. Tauch, W. Jäger, J. Kalinowski, G. Thierbach and A. Pühler, *Gene*, 1994, **145**, 69–73.
24 J. B. J. H. van Duuren, D. Wijte, A. Leprince, B. Karge, J. Puchałka, J. Wery, V. A. P. M. dos Santos, G. Eggink and A. E. Mars, *J. Biotechnol.*, 2011, **156**, 163–172.
25 H. A. de Boer, L. J. Comstock and M. Vasser, *Proc. Natl. Acad. Sci. U. S. A.*, 1983, **80**, 21–25.
26 I. Nordlund, J. Powlowski and V. Shingler, *J. Bacteriol.*, 1990, **172**, 6826–6833.
27 R. Moreno, M. Martínez-Gomariz, L. Yuste, C. Gil and F. Rojo, *J. Proteomics*, 2009, **9**, 2910–2928.
28 G. Morales, J. F. Linares, A. Beloso, J. P. Albar, J. L. Martínez and F. Rojo, *J. Bacteriol.*, 2004, **186**, 1337–1344.
29 S. Hernández-Arranz, R. Moreno and F. Rojo, *Environ. Microbiol.*, 2013, **15**, 227–241.
30 S.-G. Bang and C. Y. Choi, *J. Ferment. Bioeng.*, 1995, **79**, 381–383.
31 M. Franz, H. A. Arafat and N. G. Pinto, *Carbon*, 2000, **38**, 1807–1819.
32 A. Dąbrowski, P. Podkościelny, Z. Hubicki and M. Barczak, *Chemosphere*, 2005, **58**, 1049–1070.
33 R. Luque, C. S. K. Lin, C. Du, D. J. Macquarrie, A. Koutinas, R. Wang, C. Webb and J. H. Clark, *Green Chem.*, 2009, **11**, 193–200.
34 J. Urbanus, C. P. M. Roelands, D. Verdoes and J. H. ter Horst, *Chem. Eng. Sci.*, 2012, **77**, 18–25.

35 R. J. Madon and M. Boudart, *Ind. Eng. Chem. Fundam.*, 1982, **21**, 438–447.
36 H. S. Fogler, *Elements of Chemical Reaction Engineering*, Prentice Hall, Upper Saddle River, NJ, 4th edn, 2005.
37 M. Besson and P. Gallezot, *Catal. Today*, 2003, **81**, 547–559.
38 E. M. Karp, B. S. Donohoe, M. H. O'Brien, P. N. Ciesielski, A. Mittal, M. J. Biddy and G. T. Beckham, *ACS Sustainable Chem. Eng.*, 2014, **2**, 1481–1491.
39 E. Sjöström and R. Alén, *Analytical Methods in Wood Chemistry, Pulping, and Papermaking*, Springer Science & Business Media, 1998.
40 N. D. Bonawitz, J. Im Kim, Y. Tobimatsu, P. N. Ciesielski, N. A. Anderson, E. Ximenes, J. Maeda, J. Ralph, B. S. Donohoe, M. Ladisch and C. Chapple, *Nature*, 2014, **509**, 376–380.
41 F. Chen and R. A. Dixon, *Nat. Biotechnol.*, 2007, **25**, 759–761.
42 P. N. Ciesielski, M. G. Resch, B. Hewetson, J. P. Killgore, A. Curtin, N. Anderson, A. N. Chiaramonti, D. C. Hurley, A. Sanders, M. E. Himmel, C. Chapple, N. Mosier and B. S. Donohoe, *Green Chem.*, 2014, **16**, 2627–2635.
43 B. A. Simmons, D. Loqué and J. Ralph, *Curr. Opin. Plant Biol.*, 2010, **13**, 312–319.
44 J. J. Bozell, S. K. Black, M. Myers, D. Cahill, W. P. Miller and S. Park, *Biomass Bioenergy*, 2011, **35**, 4197–4208.
45 D. A. Fort, R. C. Remsing, R. P. Swatloski, P. Moyna, G. Moyna and R. D. Rogers, *Green Chem.*, 2007, **9**, 63.
46 T. H. Parsell, B. C. Owen, I. Klein, T. M. Jarrell, C. L. Marcum, L. J. Haupert, L. M. Amundson, H. I. Kenttämaa, F. Ribeiro, J. T. Miller and M. M. Abu-Omar, *Chem. Sci.*, 2013, **4**, 806–813.
47 M. R. Sturgeon, S. Kim, K. Lawrence, R. S. Paton, S. C. Chmely, M. Nimlos, T. D. Foust and G. T. Beckham, *ACS Sustainable Chem. Eng.*, 2014, **2**, 472–485.
48 S. Ramaswamy, H.-J. Huang and B. Ramarao, *Separation and Purification Technologies in Biorefineries*, John Wiley and Sons Ltd, Chicester, 2012.
49 W. Mu, H. Ben, A. Ragauskas and Y. Deng, *BioEnergy Res.*, 2013, **6**, 1183–1204.
50 L. N. Ornston and D. Parke, *J. Bacteriol.*, 1976, **125**, 475–488.
51 X. Chen, J. Shekiro, M. A. Franden, W. Wang, M. Zhang, E. Kuhn, D. K. Johnson and M. P. Tucker, *Biotechnol. Biofuels*, 2012, **5**, 8.
52 J. B. J. H. van Duuren, D. Wijte, B. Karge, V. A. P. Martins dos Santos, Y. Yang, A. E. Mars and G. Eggink, *Biotechnol. Prog.*, 2012, **28**, 85–92.
53 J. T. Korhonen, M. Kettunen, R. H. A. Ras and O. Ikkala, *ACS Appl. Mater. Interfaces*, 2011, **3**, 1813–1816.
54 M. Dusselier, M. Mascal and B. F. Sels, *Top Chemical Opportunities from Carbohydrate Biomass: A Chemist's View of the Biorefinery*, Springer Berlin Heidelberg, 2014, pp. 1–40.
55 W. Yu, M. D. Porosoff and J. G. Chen, *Chem. Rev.*, 2012, **112**, 5780–5817.
56 D. M. Alonso, S. G. Wettstein and J. A. Dumesic, *Chem. Soc. Rev.*, 2012, **41**, 8075–8098.
57 N. Ji, T. Zhang, M. Zheng, A. Wang, H. Wang, X. Wang and J. G. Chen, *Angew. Chem.*, 2008, **120**, 8638–8641.
58 T. Prasomsri, T. Nimmanwudipong and Y. Román-Leshkov, *Energy Environ. Sci.*, 2013, **6**, 1732–1738.
59 G. A. Somorjai, H. Frei and J. Y. Park, *J. Am. Chem. Soc.*, 2009, **131**, 16589–16605.
60 H. M. T. Galvis, J. H. Bitter, C. B. Khare, M. Ruitenbeek, A. I. Dugulan and K. P. de Jong, *Science*, 2012, **335**, 835–838.
61 D. R. Vardon, B. K. Sharma, H. Jaramillo, K. Dongwook, C. Jong Kwon, P. Ciesielski and T. J. Strathmann, *Green Chem.*, 2014, (16), 1507–1520.
62 M. Gurrath, T. Kuretzky, H. P. Boehm, L. B. Okhlopkova, A. S. Lisitsyn and V. A. Likholobov, *Carbon*, 2000, **38**, 1241–1255.
63 R. Alén, K. Niemelä and E. Sjöström, *J. Chromatogr. A*, 1984, **301**, 273–276.

